MAXIMUM POWER POINT GENETIC IDENTIFICATION FUNCTION FOR PHOTOVOLTAIC SYSTEM

Adel El Shahat
Mechatronics-Green Energy Lab., Electrical & Computer Engineering Department
The Ohio State University, USA
E-mail: adel.elshahat@ieee.org, ahmed.210@osu.edu

ABSTRACT

This paper proposes the identification of maximum power point (MPP) function for photovoltaic (PV) module using the genetic algorithm (GA). Then deduction of the required function to generate the reference values to drive the tracking system in the PV system at MPP is done with the aid of Artificial Neural Network (ANN). This function deals with the more probable situations for variable values of temperature and irradiance to get the corresponding voltage and current at maximum power. The mathematical PV module modeling depends on Schott ASE-300-DGF PV panel with the aid of MATLAB environment. The aim of this paper is to pick peaks of the power curves (maximum points). The simulation results at MPP are well depicted in 3-D figures to be used as training or learning data for the ANN model.

Keywords: *Maximum power; PV Module; Genetic Algorithm; Neural Network; MATLAB.*

1. INTRODUCTION

Photo-voltaic systems have become increasingly popular and are ideally suited for distributed systems. Many governments have provided the much needed incentives to promote the utilization of renewable energies, encouraging a more decentralized approach to power delivery systems. Recent studies show an exponential increase in the worldwide installed photovoltaic power capacity. There is ongoing research aimed at reducing the cost and achieving higher efficiency. Solar energy is the world's major renewable energy source and is available everywhere in different quantities. Photovoltaic panels do not have any moving parts, operate silently and generate no emissions. Another advantage is that solar technology is highly modular and can be easily scaled to provide the required power for different loads [1], [2]. A significant amount of fuel cell research focuses on fundamental issues of performance and cost [3-6]. Since the power harvested from the photovoltaic module is different at various operating points it is important that maximum power is obtained from the photovoltaic module [7- 9]. A PV array is usually oversized to compensate for a low power yield during winter months. This mismatching between a PV module and a load requires further over-sizing of the PV array and thus increases the overall system cost. To mitigate this problem, a maximum power point tracker (MPPT) can be used to maintain the PV module's operating point at the MPP. MPPTs can extract more than 97% of the PV power when properly optimized [7], [10]. This paper' calculations are based on practical PV module data in reference [11].

2. PV CELL MODEL

The use of equivalent electric circuits makes it possible to model characteristics of a PV cell. The method used here is implemented in MATLAB programs for simulations. The same modeling technique is also applicable for modeling a PV module. There are two key parameters frequently used to characterize a PV cell. Shorting together the terminals of the cell, the photon generated current will follow out of the cell as a short-circuit current (I_{sc}). Thus, $I_{ph} = I_{sc}$, when there is no connection to the PV cell (open-circuit), the photon generated current is shunted internally by the intrinsic p-n junction diode. This gives the open circuit voltage (V_{oc}). The PV module or cell manufacturers usually provide the values of these parameters in their datasheets [11]. The ASE-300-DGF/50 is an industrial-grade solar power module built to the highest standards. Extremely powerful and reliable, the module delivers maximum performance in large systems that require higher voltages, including the most challenging conditions of military, utility and commercial installations. For superior performance, quality and peace of mind, the ASE-300-DGF/50 is renowned as the first choice among those who recognize that not all solar modules are created equal [11]. The simplest model of a PV cell equivalent circuit consists of an ideal current source in parallel with an ideal diode. The current source represents the current generated by photons (often denoted as I_{ph} or I_L), and its output is constant under constant temperature and constant incident radiation of light. The PV panel is usually represented by the single exponential model or the double exponential model. The single exponential model is shown in fig. 1. The current is expressed in terms of voltage, current and temperature as shown in equation 1 [12].

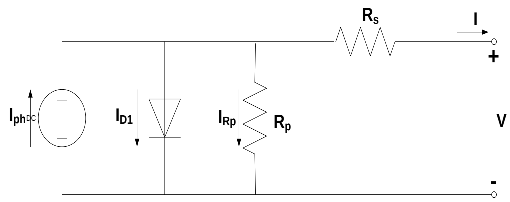

Figure 1. Single exponential model of a PV Cell

$$I = I_{ph} - I_0\left\{\exp\left[\frac{q(V+IR_s)}{AkT}\right]-1\right\} - \frac{V+IR_s}{R_p} \tag{1}$$

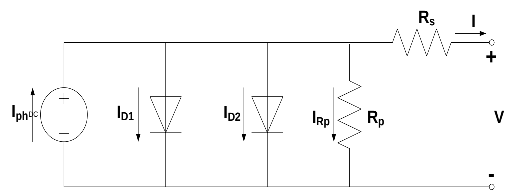

Figure 2. Double exponential model of PV Cell

$$I = I_{ph} - I_{s_1}\left\{\exp\left[\frac{q(V+IR_s)}{AkT}\right]-1\right\} - I_{s_2}\left\{\exp\left[\frac{q(V+IR_s)}{AkT}\right]-1\right\} - \frac{V+IR_s}{R_p} \tag{2}$$

Where I_{ph}: the photo generated current; I_o: the dark saturation current; I_{s1}: saturation current due to diffusion; I_{s2}: is the saturation current due to recombination in the space charge layer; I_{Rp}: current flowing in the shunt resistance; R_s: cell series resistance; R_p: the cell (shunt) resistance; A: the diode quality factor; q: the electronic charge, 1.6×10^{-19} C; k: the Boltzmann's constant, 1.38×10^{-23} J/K; and T: the ambient temperature, in Kelvin.

Eq.1 and Eq.2 are both nonlinear. Furthermore, the parameters (I_{ph}, I_{s1}, I_{s2}, R_s, R_{sh} and A) vary with temperature, irradiance and depend on manufacturing tolerance. Numerical methods and curve fitting can be used to estimate [12], [13].

There are three key operating points on the IV curve of a photovoltaic cell. They are the short circuit point, maximum power point and the open circuit point. At the open – circuit point on the IV curve, $V = V_{oc}$ and $I = 0$. After substituting these values in the single exponential equation (1) the equation can be obtained [12].

$$0 = I_{ph} - I_o\left\{\exp\left[\frac{qV_{oc}}{AkT}\right]-1\right\} - \frac{V_{oc}}{R_p} \tag{3}$$

At the short – circuit point on the IV curve, $I = I_{sc}$ and $V = 0$. Similarly, using equation (1), we can obtain.

$$I_{sc} = I_{ph} - I_o\left\{\exp\left[\frac{qI_{sc}R_s}{AkT}\right]-1\right\} - \frac{I_{sc}R_s}{R_p} \tag{4}$$

At the maximum – power point of the IV curve, we have $I = I_{mpp}$ and $V = V_{mpp}$. We can use these values to obtain the following:

$$I_{mpp} = I_{ph} - I_o\left\{\exp\left[\frac{q(V_{mpp}+I_{mpp}R_s)}{AkT}\right]-1\right\} - \frac{V_{mpp}+I_{mpp}R_s}{R_p} \tag{5}$$

The power transferred to the load can be expressed as

$$P = IV \tag{6}$$

We can estimate the diode quality factor as:

$$A = \frac{V_{mpp} + I_{mpp}R_{so} - V_{oc}}{V_T\left\{\ln(I_{sc} - \frac{V_{mpp}}{R_{sho}} - I_{mpp}) - \ln(I_{sc} - \frac{V_{oc}}{R_o}) + \frac{I_{mpp}}{I_{sc} - (V_{oc}/R_{so})}\right\}} \quad (7)$$

And

$$R_p = R_{sho} \quad (8)$$

$$I_o = (I_{sc} - \frac{V_{oc}}{R_p}).\exp(-\frac{V_{oc}}{AV_T}) \quad (9)$$

$$R_s = R_{so} - \frac{AV_T}{I_o}.\exp(-\frac{V_{oc}}{AV_T}) \quad (10)$$

$$I_{ph} = I_{sc}(1 + \frac{R_s}{R_p}) + I_o(\exp\frac{I_{sc}R_s}{AV_T} - 1) \quad (11)$$

As a very good approximation, the photon generated current, which is equal to I_{sc}, is directly proportional to the irradiance, the intensity of illumination, to PV cell [14]. Thus, if the value, I_{sc}, is known from the datasheet, under the standard test condition, G_o=1000W/m^{2}at the air mass (*AM*) = 1.5, then the photon generated current at any other irradiance, *G* (W/*m2*), is given by:

$$I_{SC|G} = (\frac{G}{G_0})I_{sc|G0} \quad (12)$$

It should be notified that, in a practical PV cell, there is a series of resistance in a current path through the semiconductor material, the metal grid, contacts, and current collecting bus [15]. These resistive losses are lumped together as a series resister (R_s). Its effect becomes very conspicuous in a PV module that consists of many series-connected cells, and the value of resistance is multiplied by the number of cells. Shunt resistance is a loss associated with a small leakage of current through a resistive path in parallel with the intrinsic device [15]. This can be represented by a parallel resister (R_p). Its effect is much less conspicuous in a PV module compared to the series resistance so it may be ignored [15], [16]. The ideality factor denoted as *A* and takes the value between one and two (as to reach the nominated characteristics) [16].

3. PHOTOVOLTAIC MODULE MODELLING

A single PV cell produces an output voltage less than 1V, thus a number of PV cells are connected in series to achieve a desired output voltage. When series-connected cells are placed in a frame, it is called as a module. When the PV cells are wired together in series, the current output is the same as the single cell, but the voltage output is the sum of each cell voltage. Also, multiple modules can be wired together in series or parallel to deliver the voltage and current level needed. The group of modules is called an array. The panel construction provides protection for individual cells from water, dust etc, as the solar cells are placed into an encapsulation of flat glass. Our case here depicts a typical connection of 216 cells that are connected in series [11]. The strategy of modelling a PV module is no different from modelling a PV cell. It uses the same PV cell model. The parameters are the all same, but only a voltage parameter (such as the open-circuit voltage) is different and must be divided by the number of cells. An electric model with moderate complexity [17] is shown in figure 3, and provides fairly accurate results. The model consists of a current source (I_{sc}), a diode (*D*), and a series resistance (R_s). The effect of parallel resistance (R_p) is very small in a single module, thus the model does not include it. To make a better model, it also includes temperature effects on the short-circuit current (I_{sc}) and the reverse saturation current of diode (I_o). It uses a single diode with the diode ideality factor set to achieve the best *I*-*V* curve match.

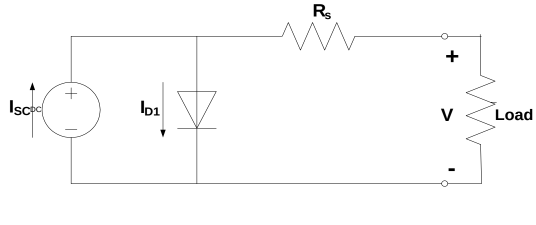

Figure 3. Equivalent circuit used in the simulations

The equation (13) describes the current-voltage relationship of the PV cell.

$$I = I_{sc} - I_o(\exp(q(\frac{V + IR_s}{AkT})) - 1) \tag{13}$$

Where: I is the cell current (the same as the module current); V is the cell voltage = {module voltage} ÷ {No. of cells in series}; T is the cell temperature in Kelvin (K).

First, calculate the short-circuit current (I_{sc}) at a given cell temperature (T):

$$I_{sc|T} = I_{sc|T_{ref}}[1 + a(T - T_{ref})] \tag{14}$$

Where: I_{sc} at T_{ref} is given in the datasheet (measured under irradiance of 1000W/m^2), T_{ref} is the reference temperature of PV cell in *Kelvin* (K), usually 298K (25^oC), a is the temperature coefficient of I_{sc} in percent change per degree temperature also given in the datasheet.

The short-circuit current (I_{sc}) is proportional to the intensity of irradiance, thus I_{sc} at a given irradiance (G) is introduced by Eq. 12.

The reverse saturation current of diode (I_o) at the reference temperature (T_{ref}) is given by the equation (15) with the diode ideality factor added:

$$I_0 = \frac{I_{sc}}{(\exp(\frac{qV_{oc}}{AkT}) - 1)} \tag{15}$$

The reverse saturation current (I_o) is temperature dependant and the I_o at a given temperature (T) is calculated by the following equation [17].

$$I_{0|T} = I_{0|T_{ref}}(\frac{T}{T_{ref}})^{\frac{3}{A}} \exp(\frac{-qE_g}{Ak}(\frac{1}{T_{ref}} - \frac{1}{T_{ref}})) \tag{16}$$

The diode ideality factor (A) is unknown and must be estimated. It takes a value between one and two; however, the more accurate value is estimated by curve fitting [17] also, it can be estimated by try and error until accurate value achieved. E_g is the Band gap energy (1.12 V (Si); 1.42 (GaAs); 1.5 (CdTe); 1.75 (amorphous Si)).

The series resistance (R_s) of the PV module has a large impact on the slope of the *I-V* curve near the open-circuit voltage (V_{oc}), hence the value of R_s is calculated by evaluating the slope dI/dV of the *I-V* curve at the V_{oc} [17]. The equation for R_s is derived by differentiating the I-V equation and then rearranging it in terms of R_s *as* introduced in equation (17).

$$R_s = -\frac{dV}{dI}\Big|_{Voc} - \frac{AkT/q}{I_0 \exp(\frac{qV_{oc}}{AkT})} \tag{17}$$

Where: $\frac{dV}{dI}\Big|_{V_{oc}}$ is the slope of the *I-V* curve at the V_{oc} (using the I-V curve in the datasheet then divide it by the number of cells in series); V_{oc} is the open-circuit voltage of cell (Dividing V_{oc} in the datasheet by the number of cells in series).

Finally, the equation of *I-V* characteristics is solved using the Newton's method for rapid convergence of the answer, because the solution of current is recursive by inclusion of a series resistance in the model [17]. The Newton's method is described as:

$$x_{n+1} = x_n - \frac{f(x_n)}{f'(x_n)} \tag{18}$$

Where: $f'(x)$ is the derivative of the function, $f(x) = 0$, x_n is a present value, and x_{n+1} is a next value.

$$f(I) = I_{sc} - I - I_o(\exp(q(\frac{V + IR_s}{AkT})) - 1) = 0 \tag{19}$$

By using the above equations the following output current (I) is computed iteratively.

$$I_{n+1} = I_n - \frac{I_{sc} - I_n - I_o(\exp(q(\frac{V + I_n R_s}{AkT})) - 1)}{-1 - I_o(\frac{qR_s}{AkT})\exp(q(\frac{V + I_n R_s}{AkT}))} \quad (20)$$

The following little figures at various module temperatures simulated with the MATLAB model for our PV module are shown with the maximum power points identified on them. After that, a more powerful tool is presented (Genetic Algorithm) to be used for finding the MPPs over most probable range.

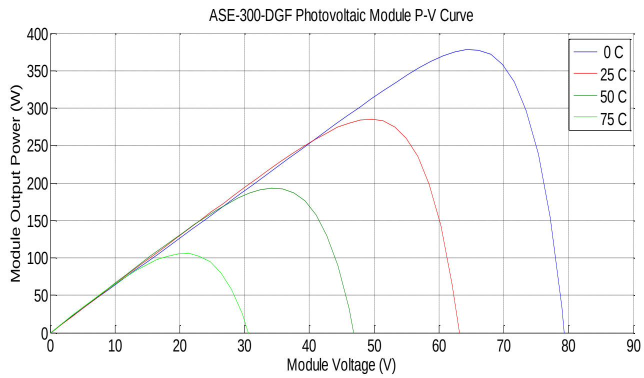

Figure 4. P-V curves at (1KW/m^2; 0, 25, 50, 75^{o}C)

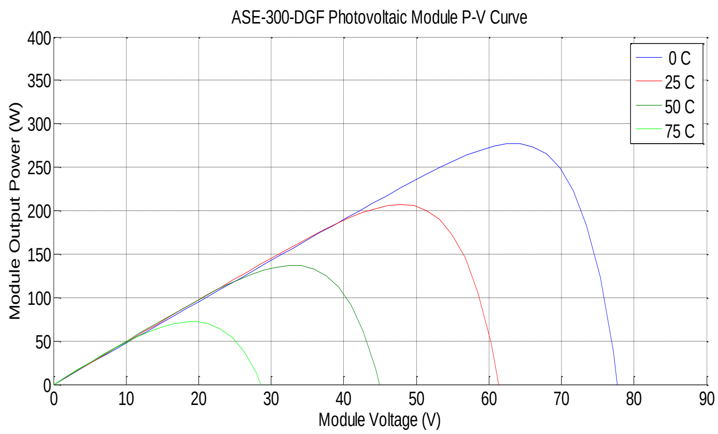

Figure 5. P-V curves (0.75KW/m^2; 0, 25, 50, 75^{o}C)

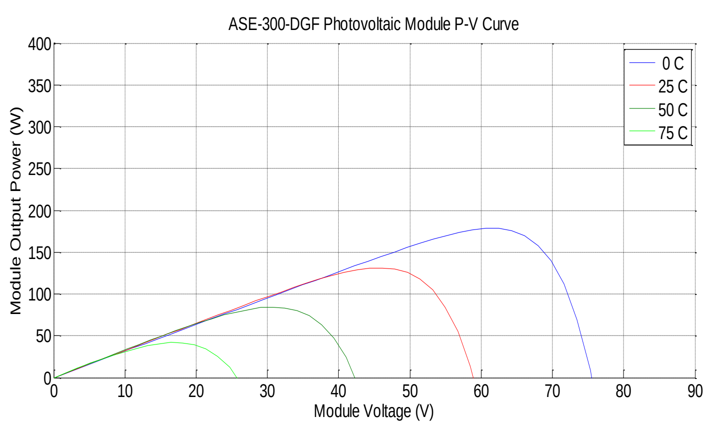

Figure 6. P-V curves (0.50KW/m^2; 0, 25, 50, 75^{o}C)

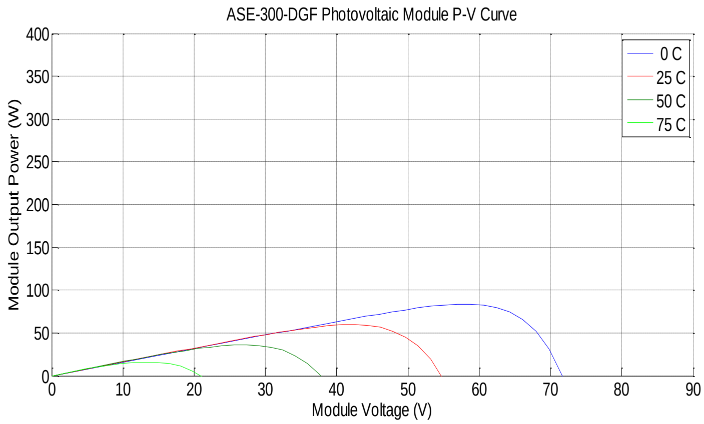

Figure 7. P-V curves (0.25KW/m^2; 0, 25, 50, 75^{o}C)

From the above figures, it is clear that there is a maximum point at each irradiance value with the temperature value. The coming stage presents the genetic algorithm function to identify this maximum point for more wide range than before then using the facility of ANN to deduce the required drive equation.

4. GENETIC ALGORITHM

The genetic algorithm is a method for solving both constrained and unconstrained optimization problems that is based on natural selection, the process that drives biological evolution. The genetic algorithm repeatedly modifies a population of individual solutions. At each step, the genetic algorithm selects individuals at random from the current population to be parents and uses them to produce the children for the next generation. Over successive generations, the population "evolves" toward an optimal solution. We can apply the genetic algorithm to solve a variety of optimization problems that are not well suited for standard optimization algorithms, including problems in which the objective function is discontinuous, non - differentiable, stochastic, or highly nonlinear [18 – 23].

The genetic algorithm uses three main types of rules at each step to create the next generation from the current population:

- Selection rules select the individuals, called parents, which contribute to the population at the next generation.
- Crossover rules combine two parents to form children for the next generation.
- Mutation rules apply random changes to individual parents to form children.

Our genetic trial uses the following MATLAB prescribed terminologies:

Population type: Double Vector with Populations size = 20; Creation function, Initial population, Initial Score, and Initial range: Default; Fitness scaling: Rank; Selection function: Stochastic uniform Reproduction; Elite Count: Default (3), Crossover fraction: Default (0.8); Mutation function: Adaptive feasible (due to its benefits); Crossover function: Scattered Migration; Direction: Forward, Fraction: Default (0.2), Interval: Default (20); Stopping criteria (Defaults): Generations: 100, Time limit: Inf., Fitness limit: Inf., Stall generations: 50, Stall time limit: Inf., Function Tolerance: 1e-6, nonlinear constraint tolerance: 1e-6.

Also, this technique is used before by the same authors in the field of green energy in [24-26].

4.1 MAXIMUM POWER GA FUNCTION

The aim of this function is to pick the peaks of PV power curves shown before; as the objective function and out two variables as arguments x(1), and x(2) (V_{mp}, and I_{mp}).

This efficient function is implemented by maximizing the power with the voltage and current as optimizing variables, and with bounds for them by the values of V_{oc}, and I_{sc} from the PV module data sheet, also with nonlinear constraints with the aid of V_{oc}, and I_{sc} obtained from I-V curves for each irradiances, and temperatures values. Both the objective function and constraint function are implemented using the previous modeling relations in the form of MATLAB m-files.

Function MPP = f (x)

MPP = x(1) * x(2) (21)

Function Constraints:

This optimizing variable (x(1)) is bounded by [0 $V_{ocDataSheet}$].

This optimizing variable (x(2)) is bounded by [0 $I_{scDataSheet}$].
The nonlinear constraint:
Function [c,ceq] = *f* (x)

$$c = [z1 - V_{ocModule(For\ Each\ Irradiance\ \&\ Temperature\ Values)};\ z2 - I_{scModule(For\ Each\ Irradiance\ \&\ Temperature\ Values)}\ ] \quad (22)$$

ceq = [ ]

4.2 GENETIC ALGORITHM RESULTS

Finally, a set of 3 D figures are proposed to cover the most probable situations at various irradiance, various temperature with the current, the voltage, and the power at the desired maximum power. These surface faces relations will be considered later as the learning or training data for the ANN model. The following figures cover the most probable range for both irradiance (0.05:1 kW/m^2) and temperature (0:75 °C).

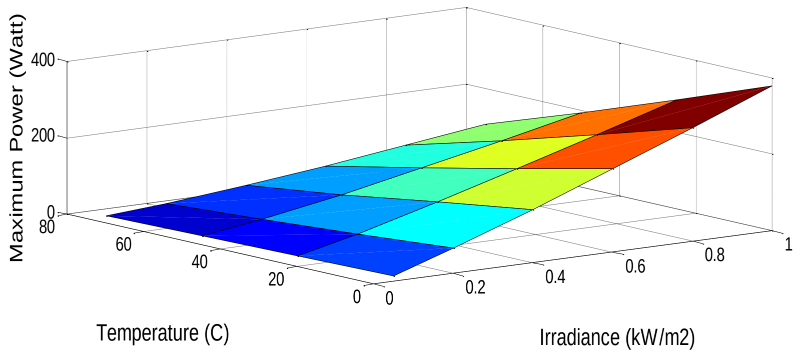

Figure 8. Maximum Power relation with Irradiance and Temperature

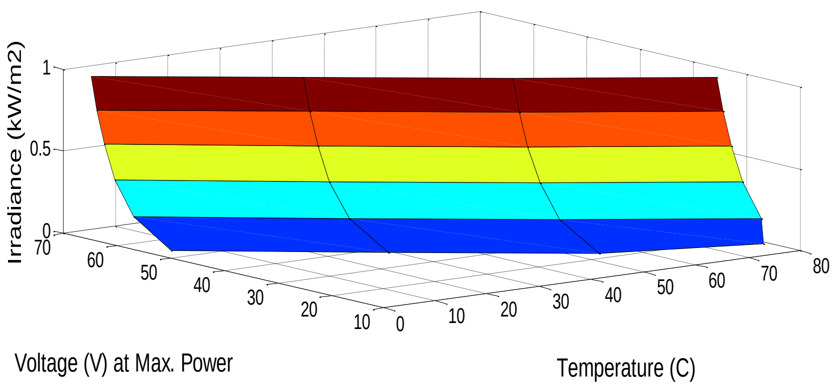

Figure 9. Voltage at Maximum Power relation with Irradiance and Temperature

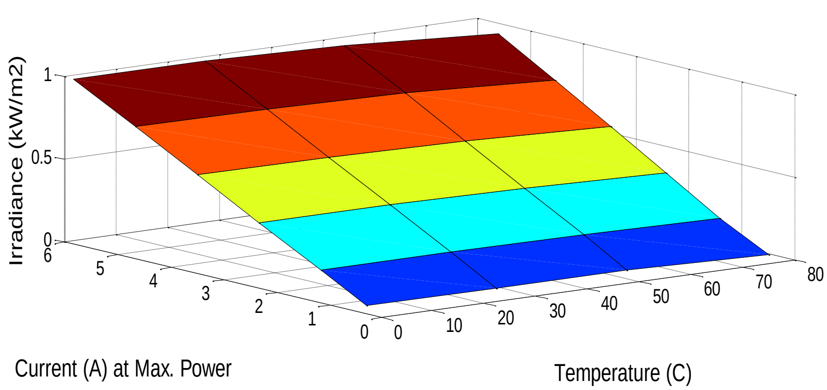

Figure 10. Current at Maximum Power relation with Irradiance and Temperature

The neural network has the ability to deal with all previous relations as surface or mapping face, due to this technique ability for interpolation between points with each other and also curves.

5. ANN PV GA FUNCTION WITH ITS REGRESSION FUNCTION

This model uses the ANN technique with back-probagation technique which used, described and verified before in the field of renewable energy like in [27-33] for the same author. This model uses the previous 3D graphs illustrated before as training or learning data for input and desired target. The inputs in this model are the Irradiance and Temperature; the outputs are: Module Voltage, and Current at maximum Power. This model with its hidden and output layers' suitable neurons numbers is depicted in fig. 11. Also, the training state is presented in fig. 12, and 13 respectively.

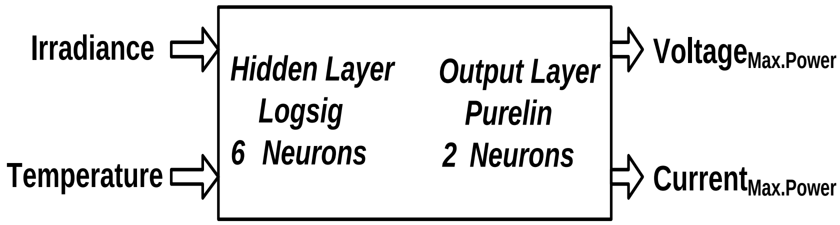

Figure 11. ANN Genetic PV Module Model at Maximum power

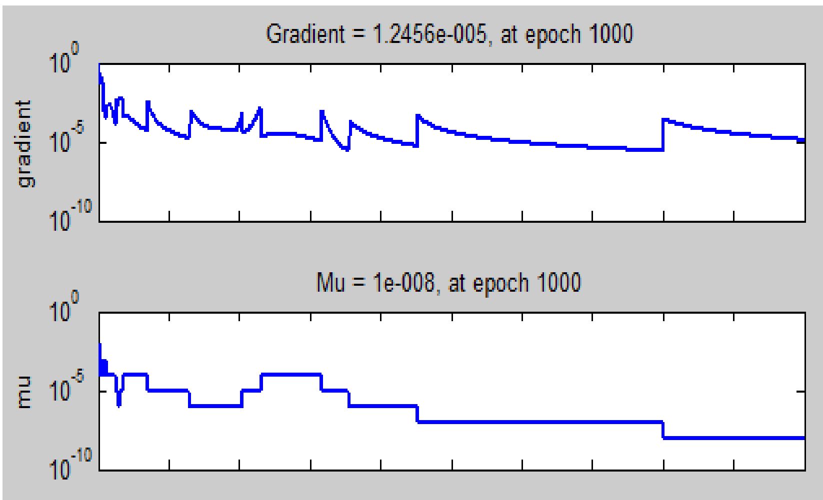

Figure 12. Training State

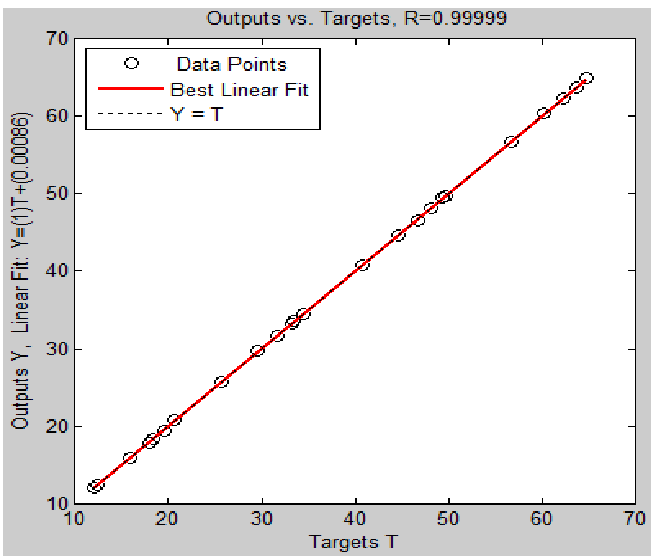

Figure 13. Comparisons samples of actual and ANN-predicted values for Voltage

The regression neural network function is deduced as follow:
The normalized inputs G_n: (Normalized Irradiance); T_n: (Normalized Temperature) are:

$$G_n = (G - 0.5083) / (0.3368) \quad (23)$$

$$T_n = (T - 37.5000) / (28.5520) \quad (24)$$

The following equations lead to the required derived outputs equations.

$$\begin{aligned} E1 &= 8.8013\, G_n + 32.6047\, T_n - 31.3610 \\ F1 &= 1 / (1 + \exp(-E1)) \end{aligned} \quad (25)$$

$$\begin{aligned} E2 &= 0.1741\, G_n - 0.2375\, T_n - 0.0988 \\ F2 &= 1 / (1 + \exp(-E2)) \end{aligned} \quad (26)$$

$$\begin{aligned} E3 &= 0.0580\, G_n + 6.2039\, T_n + 1.0561 \\ F3 &= 1 / (1 + \exp(-E3)) \end{aligned} \quad (27)$$

$$\begin{aligned} E4 &= -0.0352\, G_n - 13.9139\, T_n - 4.7855 \\ F4 &= 1 / (1 + \exp(-E4)) \end{aligned} \quad (28)$$

$$\begin{aligned} E5 &= -2.3454\, G_n + 0.0302\, T_n - 8.5850 \\ F5 &= 1 / (1 + \exp(-E5)) \end{aligned} \quad (29)$$

$$\begin{aligned} E6 &= -0.2908\, G_n - 16.7000\, T_n - 19.6496 \\ F6 &= 1 / (1 + \exp(-E6)) \end{aligned} \quad (30)$$

The normalized outputs are:

$$V_n = -0.6907\, F1 + 3.0723\, F2 + 2.2439\, F3 + 3.2258\, F4 - 123.3601\, F5 + 0.4641\, F6 - 3.9162 \quad (31)$$

$$I_n = 0.1583\, F1 + 22.0215\, F2 + 36.2987\, F3 + 36.3581\, F4 + 1.2441\, F5 - 3.4176\, F6 - 45.3856 \quad (32)$$

The un- normalized out puts

$$V = 17.3087\, V_n + 37.2067 \quad (33)$$

$$I = 1.9128\, I_n + 2.7979 \quad (34)$$

6. CONCLUSION

Due to the importance of PV systems especially in green energy field, this paper introduces an efficient identification method for maximum power point (MPP) function for photovoltaic (PV) module using the genetic algorithm (GA). The required function to generate the reference values to drive the tracking system in the PV system at MPP is done with the aid of Artificial Neural Network (ANN). This function uses the most probable situations for variable values of temperature and irradiance to get the corresponding voltage and current at maximum power. The mathematical PV module modelling depends on Schott ASE-300-DGF PV panel with the aid of MATLAB environment. The aim of this paper is to pick peaks of the power curves (maximum points) to make the sun tracker works efficiently. The simulation results at MPP are well depicted in 3-D figures to be used as training or learning data for the ANN model. Finally, the ANN regression function for this unit is introduced to be used directly without operating the neural model each times.

7. ACKNOWLEDGMENT

I would like to thank Ms. Shaza M. Abd Al Menem for her effort in this research editing.

REFRENCES

[1] [s.n.], \Trends in photovoltaic applications. survey report of selected iea countries between 1992 and 2006.
[2] T. Markvart and L. Castaner, Practical Handbook of Photovoltaics, Fundamentals and Applications. Elsevier, 2003.
[3] Ahluwalia, R., Wang, X., Lasher, S., Sinha, J., Yang, Y., and Sriramulu, S. "Performance of automotive fuel cell systems with nanostructured thin film catalysts." Proceedings of the 2007 Fuel Cell Seminar and Exposition, San Antonio, TX, 2007.
[4] Meimei Guo, Baijun Liu, Long Li, Chang Liu, LifengWang, Zhenhua Jiang, "Preparation of sulfonated poly(ether ether ketone)s containing amino groups/epoxy resin composite membranes and their in situ crosslinking for application in fuel cells," Journal of Power Sources 195 (2010) 11–20
[5] Tauqir A. Sherazi, Michael D. Guiver, David Kingston, Shujaat Ahmad, M. Akram Kashmiri, Xinzhong Xue, "Radiation-grafted membranes based on polyethylene for direct methanol fuel cells," Journal of Power Sources 195 (2010) 21–29

[6] Xiu Qing Xing, KahWai Lum, Hee Joo Poh, Yan LingWu, "Optimization of assembly clamping pressure on performance of proton-exchange membrane fuel cells," Journal of Power Sources 195 (2010) 62–68

[7] K. Hussein, I. Muta, T. Hoshino, and M. Osakada, "Maximum photovoltaic power tracking: an algorithm for rapidly changing atmospheric conditions," Generation, Transmission and Distribution, IEE Proceedings-, vol. 142, pp. 59–64, Jan 1995.

[8] D. Hohm and M. Ropp, "Comparative study of maximum power point tracking algorithms using an experimental, programmable, maximum power point tracking test bed," Photovoltaic Specialists Conference, 2000. Conference Record of the Twenty-Eighth IEEE, pp. 1699–1702, 2000.

[9] D. Sera, R. Teodorescu, and P. Rodriguez, "Pv panel model based on datasheet values," Industrial Electronics, 2007. ISIE 2007. IEEE International Symposium on, pp. 2392–2396, June 2007.

[10] Hohm, D. P. & M. E. Ropp "Comparative Study of Maximum Power Point Tracking Algorithms" Progress in Photovoltaics: Research and Applications November 2002, page 47-62

[11] Schott ASE-300-DGF PV panel data sheet. Source (Affordable Solar website);http://www.affordable-solar.com/admin/product_doc/Doc_pd-00-009-c_ase_300_20080328114646.pdf

[12] Ali Keyhani, Mohammad N. Marwali, and Min Dai, "Integration of Green and Renewable Energy in Electric Power Systems," Wiley, January 2010

[13] Masters, Gilbert M. Renewable and Efficient Electric Power Systems John Wiley & Sons Ltd, 2004

[14] Messenger, Roger & Jerry Ventre Photovoltaic Systems Engineering 2nd Edition CRC Press, 2003

[15] Castañer, Luis & Santiago Silvestre Modelling Photovoltaic Systems, Using PSpice John Wiley & Sons Ltd, 2002

[16] Green, Martin A. Solar Cells; Operating Principles, Technology, and System Applications Prentice Hall Inc., 1982

[17] Walker, Geoff R. "Evaluating MPPT converter topologies using a MATLAB PV model" Australasian Universities Power Engineering Conference, AUPEC '00,Brisbane, 2000

[18] A. R. Conn, Gould N. I. M., and Toint Ph. L. "A Globally Convergent Augmented Lagrangian Algorithm for Optimization with General Constraints and Simple Bounds," SIAM Journal on Numerical Analysis, Volume 28, Number 2, 1991, pages 545–572.

[19] A. R. Conn, Gould N. I. M., and Toint Ph. L. "A Globally Convergent Augmented Lagrangian Barrier Algorithm for Optimization with General Inequality Constraints and Simple Bounds. Mathematics of Computation," Volume 66, Number 217, pages 261– 288.

[20] D.E Goldberg, Genetic Algorithms in Search Optim. and Machine Learning. Addison Wesley; 1989.

[21] G. Rudolph, 1994 "Convergence Analysis of Canonical Genetic Algorithms," IEEE Trans. On N.N.; Vol. 5; No. 1; Jan. 1994, PP. 96-101.

[22] H. Holland, "Adaptation in Natural and Artificial Systems," Ann Arbor, Univ. of Michigan Press, 1995.

[23] G. Cvetkovski, Petkovska L., Cundev M. and Gair S. " Mathematical model of a permanent magnet axial field synchronous motor for GA optimisation," in Proc. ICEM'98, Vol. 2/3, 1998, pp. 1172-1177.

[24] A. El Shahat, A. Keyhani, and H. El Shewy, "Spacecraft Flywheel High Speed PM Synchronous Motor Design (Classical & Genetic)", Journal of Theoretical and Applied Information Technology, March 2010, Vol. 13, No. 1, pp. 83-100.

[25] Adel El Shahat, and Hamed El Shewy, "PM Synchronous Motor Genetic Algorithm Performance Improvement for Renewable Energy Applications", MDGEN11, Accepted in the International Conference on Millennium Development Goals (MDG): Role of ICT and other technologies December 27 ‒ 29, 2009 in Chennai, India.

[26] Adel El Shahat, and Hamed El Shewy, "PM Synchronous Motor Genetic Algorithm Performance Improvement for Green Energy Applications", Paper ID: X792, Accepted in 2nd International Conference on Computer and Electrical Engineering (ICCEE 2009); Dubai, UAE, December 28 - 30, 2009.

[27] A. El Shahat, and H. El Shewy, "PM Synchronous Motor Control Strategies with Their Neural Network Regression Functions", Journal of Electrical Systems (JES), Vol. 5, Issue 4, Dec. 2009.

[28] Adel El Shahat and Hamed El Shewy, "High Fundamental Frequency PM Synchronous Motor Design Neural Regression Function", Journal of Electrical Engineering, Vol. 10 / 2010 – Edition 1, Article 10.1.14.

[29] Adel El Shahat, and Hamed El Shewy, "High Speed Synchronous Motor Basic Sizing Neural Function for Renewable Energy Applications", MDGEN05, Accepted in the International Conference on Millennium Development Goals (MDG): Role of ICT and other technologies December 27 ‒ 29, 2009 in Chennai, India.

[30] Adel El Shahat, and Hamed El Shewy, "High Speed PM Synchronous Motor Basic Sizing Neural Regression Function for Renewable Energy Applications", Paper ID: X304, Accepted in 2nd International Conference on Computer and Electrical Engineering (ICCEE 2009); Dubai, UAE, December 28 - 30, 2009.

[31] A. El Shahat, "Generating Basic Sizing Design Regression Neural Function for HSPMSM in Aircraft" EP-127, 13th International Conference on Aerospace Science & Aviation Technology, May 26 – 28, 2009, ASAT 2009 – Military Technical College, Cairo, Egypt.

[32] El Shahat, A and El Shewy, H, "Neural Unit for PM Synchronous Machine Performance Improvement used for Renewable Energy", Ref: 93, The Third Ain Shams University International Conference on Environmental Engineering (Ascee- 3), April 14-16 2009, Cairo, Egypt.

[33] A. El Shahat, H. El Shewy, "Neural Unit for PM Synchronous Machine Performance Improvement used for Renewable Energy", Paper Ref.: 910, Global Conference on Renewable and Energy Efficiency for Desert Regions (GCREEDER2009), Amman, Jordan.